A shear-induced network of aligned wormlike micelles in a sugar-based molecular gel. From gelation to biocompatibility assays

Juliette Fitremann, Barbara Lonetti, Emiliano Fratini, Isabelle Fabing, Bruno Payre, Christelle Boulé, Isabelle Loubinoux, Laurence Vaysse, Luis Oriol

Citation: Fitremann, J.; Lonetti, B.; Fratini, E.; Fabing, I.; Payré, B.; Boulé, C.; Loubinoux, I.; Vaysse, L.; Oriol, L. A Shear-Induced Network of Aligned Wormlike Micelles in a Sugar-Based Molecular Gel. From Gelation to Biocompatibility Assays. Journal of Colloid and Interface Science ***2017****, 504, 721–730. https://doi.org/10.1016/j.jcis.2017.06.021.*

A shear-induced network of aligned wormlike micelles in a sugar-based molecular gel. From gelation to biocompatibility assays

Juliette Fitremann*[a], Barbara Lonetti[a], Emiliano Fratini[b], Isabelle Fabing[c], Bruno Payré[d], Christelle Boulé[e], Isabelle Loubinoux[f], Laurence Vaysse[f], Luis Oriol[g]

a CNRS - Université de Toulouse III Paul Sabatier, Laboratoire des Interactions Moléculaires et Réactivité Chimique et Photochimique (IMRCP, UMR 5623), Bat 2R1, 118 Route de Narbonne, 31062 Toulouse Cedex 9, France.
b Department of Chemistry "Ugo Schiff" and CSGI, University of Florence, via della Lastruccia 3-Sesto Fiorentino, I-50019, Florence, Italy.
c CNRS UMR 5068, LSPCMIB, Université de Toulouse, Université Paul Sabatier, 118 Route de Narbonne, 31062 Toulouse cedex 9, France.
d Centre de Microscopie Electronique Appliquée à la Biologie (CMEAB), Faculté de Médecine Rangueil, Université de Toulouse III Paul Sabatier, Bâtiment A5, R.D.C., 133 Route de Narbonne, 31400 Toulouse, France.
e Université Claude Bernard UCBL Lyon1, Service de Prestations CTμ EZUS, Bâtiment Darwin B, 5 rue Raphaël Dubois, 69622 Villeurbanne Cedex, France.
f TONIC, Toulouse NeuroImaging Center, Université de Toulouse, Inserm, UPS, France.
g Instituto de Ciencia de Materiales de Aragon (ICMA),Universidad de Zaragoza-CSIC, Dpto. Quimica Organica, Facultad de Ciencias, Pedro Cerbuna 12, 50009 Zaragoza, Spain.

A new low molecular weight hydrogelator with a saccharide (lactobionic) polar head linked by azide-alkyne click chemistry was prepared in three steps. It was obtained in high purity without chromatography, by phase separation and ultrafiltration of the aqueous gel. Gelation was not obtained reproducibly by conventional heating-cooling cycles and instead was obtained by shearing the aqueous solutions, from 2wt% to 0.25 wt%. This method of preparation favored the formation of a quite unusual network of interconnected large but thin 2D-sheets (7 nm-thick) formed by the association side-by-side of long and aligned 7 nm diameter wormlike micelles. It was responsible for the reproducible gelation at the macroscopic scale. A second network made of helical fibres with a 10-13 nm diameter, more or less intertwined was also formed but was scarcely able to sustain a macroscopic gel on its own. The gels were analysed by TEM (Transmission Electronic Microscopy), cryo-TEM and SAXS (Small Angle X-Ray Scattering). Molecular modelling was also used to highlight the possible conformations the hydrogelator can take. The gels displayed a weak and reversible transition near 20°C, close to room temperature, ascribed to the wormlike micelles 2D-sheets network. Heating over 30°C led to the loss of the gel macroscopic integrity, but gel fragments were still observed in suspension. A second transition near 50°C, ascribed to the network of helical fibers, finally dissolved completely these fragments. The

gels showed thixotropic behaviour, recovering slowly their initial elastic modulus, in few hours, after injection through a needle. Stable gels were tested as scaffold for neural cell line culture, showing a reduced biocompatibility. This new gelator is a clear illustration of how controlling the pathway was critical for gel formation and how a new kind of self-assembly was obtained by shearing.

Keywords: supramolecular; gel; self-assembly; carbohydrate amphiphile; saccharide; triazole; fiber; fibre; cylindrical micelle; shear; cell culture; biomaterial; LMWG; low molecular weight gelator.

Electronic Supplementary Information: Experimental section, extra electronic microscopy data, HLPC-MS chromatograms, NMR spectra.

Graphical abstract

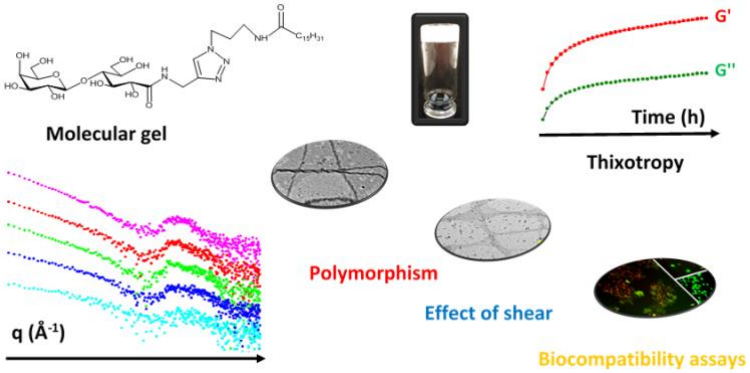

Introduction

Low molecular weight (LMW) hydrogelators provide an alternative family of gelling agents compared with polymers, leading to soft materials with possible applications in the field of wet materials, switchable gels, controlled release or uptake, cell culture. LMW gelators belong to different structural families (peptides, cholesteryl, nucleobase or sugar amphiphiles, etc…) and the now quite large amount of work done on these self-assembling molecules has been well reported in several reviews [1–21]. We are more especially interested in sugar-derived molecular gelators (see the recent review on this family of gelators and the following references for the most recent works [22–50]). Sugar gelators provide generally a neutral hydrophilic polar head, with a low sensitivity to temperature changes on the contrary to PEG amphiphiles. In the context of biological applications, carbohydrate derived hydrogels will interact differently with biomolecules or cells compared with PEG or peptide derived gelators, notably by mimicking to some extent the saccharidic components of the glycocalix, composed of glycoproteins and glycolipids [22].

From a practical point of view, simple, rapid and cheap syntheses are essential when considering sugar-based LMW hydrogelators applications. In former results, a family of hydrogelators based on a disaccharide head has been described. It has been shown that the presence of a triazole linker enhanced gelation, but the synthetic pathway consisted of six steps [23–26]. Other amphiphilic molecules with close structures (namely, a sugar head, triazole linkers, and a fatty chain) have been described as well, including hydrogelators [27–29], organogelators [30] and micelles [31–33], all of them involving also

protection-deprotection multistep synthesis and purification by chromatography. In this work, a new gelator inspired from these structures has been prepared with a simpler synthetic route with only three steps starting from lactobionic acid as the polar head (Scheme 1). Another important aspect in the field of LMW hydrogelators is to control in a precise manner the supramolecular structure sustaining the gel. In the case of very flexible molecules many conformations are possible. It can give rise to polymorphism. Polymorphism is the main cause for the lack of reproducible gelation [34–37]. Accordingly, the importance of controlling the conditions of the self-assembly in order to reach a reproducible final state, with the related macroscopic properties, has been well pointed out in several papers. But it still remains underestimated, quite unexplored and not well controlled [38–42]. Compound **3** is a typical example of such a situation. Its gelation behaviour appeared more complex than expected and gave the opportunity to explore the effect of different pathways for the gel preparation. The self-assembled structures have been elucidated by electronic microscopy and Small Angle X-Ray Scattering (SAXS). The rheology and thermal transitions of the gel have also been studied. Finally, the results related to the use of these gels for cell culture are briefly discussed.

Results and discussion

1. Preparation of the gelator

An easy access to the sugar based gelator **3** is represented in Scheme 1. The gelator was obtained in three synthetic steps and was purified without chromatography. The fatty chain **1** was purified by recrystallization (yield 60%) while the product **2** was obtained nearly pure by extraction and was used without further purification in the next step. After the azide-alkyne "click chemistry" step, leading to the compound **3**, the unreacted and sparingly soluble azide was discarded by centrifugation. The cleared and concentrated reaction medium was diluted in water and allowed to rest for several hours, until a gel was formed. The gel was purified by ultrafiltration or dialysis, removing water soluble by-products. Analysis of the filtrate showed that about 5% of the gelator went out through the membrane after four volumes and 24h of ultrafiltration, evidencing a low proportion of free molecules. A last step of filtration in methanol enabled to get rid of traces of the azide remaining after ultrafiltration. After this sequence, the gelator was pure (yield 76%, freeze-dried), according to NMR, HPLC-MS chromatograms (see Fig. SI-11-13). Residual copper was analysed and it did not exceed 300 ppm (0.3µg/mg) when ultrafiltration was performed in the presence of EDTA.

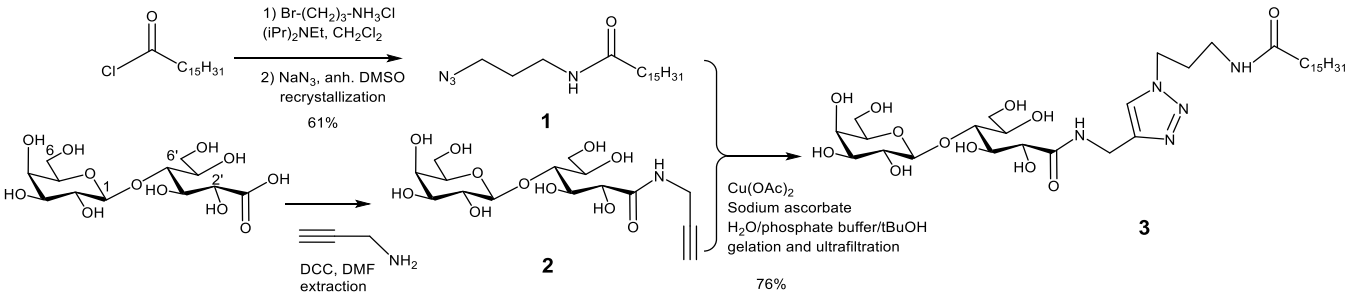

*Scheme 1. Synthetic scheme for the preparation of the gelator **3***

2. Gelation

Gelation of the gelator **3** was at first quite puzzling. The crude product coming directly from the reaction mixture and diluted in water (after solvent removal) provided directly the hydrogel within 24 hours of standing. Conversely, the purified and dried samples gave a non-reproducible gelation behaviour. The usual method consisting in heating the solution until solubilisation followed by cooling did not lead to reproducible gelation, whatever the concentration (from 0.1 to 2%wt). It has been checked that this effect was not the result of the degradation of the molecule. It was still intact after heating for 4 hours at 60°C (see SI-12). Heating may favour a change of intra or intermolecular bonding leading to insoluble aggregates instead of gel. Concentrated samples at 2% usually provided gels but sometimes, viscous turbid solutions or suspensions are obtained instead of gels. And conversely, it happened that very diluted samples (0,3 to 0.1%) formed spontaneously gels, but in a non-reproducible manner (see SI-4). Sonication did not help gelation (see SI-7), and the purification method did not appeared either as the key parameter for gelation.

Finally, it was observed that shearing was a key factor for triggering the gelation reproducibly for this compound. A reliable gelation procedure was then set up. A 2% suspension in water was prepared and the hydration and solubilisation of the solid was allowed for few hours (2 to 24h). It provided a heterogeneous suspension containing non-cohesive white cotton-like gels fragments. The sample was then sheared through a needle until an homogeneous opalescent solution was obtained. Finally, the sample was let resting for gelation at room temperature (20°C or lower). A turbid gel, macroscopically homogenous was formed within c.a. 2 hours. It can be turned upside down (Figure 6 and SI-1 "Gelation"). Additional cycles of shear/rest were sometimes applied to improve gelation and homogeneity. The gel was also diluted stepwise up to 0.25% by shearing, ranking the molecule among super-hydrogelators. Time also appeared as a key factor for gelation, notably because of the solubilisation kinetics, but also because the gel appeared to be thixotropic, but with a slow recovery (see section E-rheology).
The benefit of shear on gelation has already been observed in few examples of organogels [43,44], hydrogels [45,46] and micellar solutions [47]. Shearing can affect, first, the distribution of the aggregates in the solution and can help to get a more homogeneous distribution of the growing self-assemblies. The shear can also affect the shape of the self-assemblies, by lengthening the aggregates or even by changing the growth pathway and thus, the polymorph formed, as it has been observed in the examples cited above. Shearing can also provide foam, namely a large air-water interface on which the amphiphilic molecules can absorb and organize before coalescence. The walls of the needle used to shear may also act as an interface for organizing the molecules. In our case, the effect of shear on the gels of **3** will be discussed in the light of SAXS, electronic microscopy and rheology (see section D).

Alternative preparation with DMSO as cosolvent (DMSO/H2O 1/2 v/v) was less challenging. Gels with good mechanical strength were obtained easily by the conventional heating-cooling method (see SI-8 for TEM). They were rinsed several times to remove DMSO, providing purely aqueous gels. The solvent change did not alter their mechanical properties and stability, during and after rinsing. However, introducing a solvent for gel formation is often undesirable, notably for biocompatibility assays. For this reason, unravelling the conditions for gel formation in pure water, as described above, was more challenging, but necessary.

3. Thermal transitions

The thermal transitions have been studied by DSC and by visual inspection of the sample (Figure 1). For a gel at 2wt% prepared by shearing, two transitions were observed. A first transition starting at 17°C and ending at 30°C (5 J/g with respect to the gelator; 0.2 J/g if considering the entire gel) corresponded to the loss of the macroscopic gel integrity, but large gel domains were still visible floating in a liquid phase. A second transition starting at 35°C and ending at 55°C fitted with the complete disappearance of all macroscopic gelled fragments. Over 55°C, the sample was completely liquid and clear. Both transitions were partly reversible, and the gel was recovered after 30 min at 5°C. However, repeated heating over 60°C caused the formation of a precipitate and prevented any recovery of the gel state.

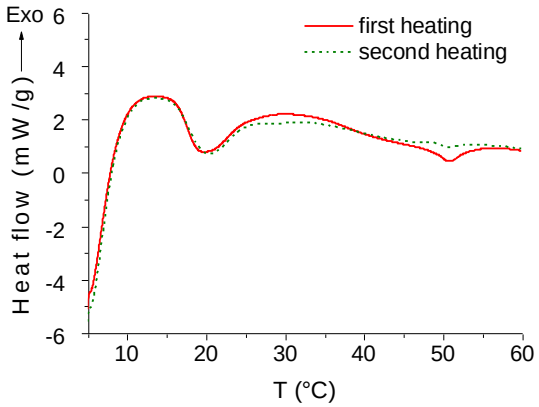

Figure 1. Two consecutive heating curves of hydrogel at 2wt% prepared by shearing (2°C/min).

4. Morphology

The morphology of the self-assembled aggregates has been observed with different microscopic techniques and detailed by SAXS.

Microscopy. In a 2wt% gel obtained by shearing, two morphologies were mainly observed by TEM and cryo-TEM: intertwined helical fibres (Figure 2-e-f-g), and large and flexible ribbons or sheets (Figure 2-a-b-c). Both of them have a substructure. The wide helical fibres are made by the intertwining of thinner 10-13 nm "single" helical fibres. These 10-13 nm fibres themselves resulted from the stacking of structures with a 5-6 nm spacing. These structures are pairs of two bright bands (≈2.5 nm) separated by a darker one, thus can be interpreted as bilayers (Figure 2-g and SAXS). Sheets are made of long structures with 7 nm width organized in parallel side-by-side on a long range, over several millimetres (Figure 2-b). These long structures typically look like long cylindrical, wormlike micelles. Concentration played a role in the formation of the sheets. At high concentration (2wt%), sheets are the main structures observed (and confirmed by SAXS). Conversely, at lower concentration, helical fibres are the main ones. The latter are generally not able to sustain a gel. In the 2 wt% and sheared gels of Figures 2-a, b, c, helical fibres can however be seen (Figure 2-e), but they are a minority population. Shear also played a role. Without shear, the structures formed at 2wt% looked like short platelets by TEM (SI-2).

They are too short to sustain a intertwined network and the sample often did not gel. After shear, the intertwined long sheet-like structures are observed. These ones are able to form a persistent network throughout the sample and are able to sustain a gel. The more the sample is sheared, the more extended is this interconnected sheets structure. Besides, a population of short and randomly arranged wormlike micelles with 6-7 nm width was also observed by cryo-TEM (this population was the main one just after shearing but was still observed, to a lesser extent, after resting as well) (Figure 2-d).

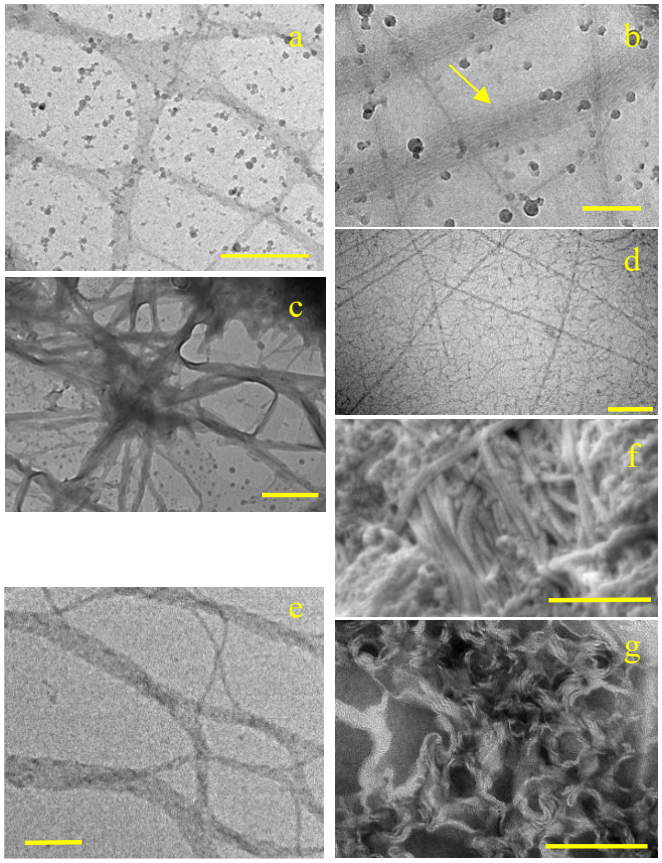

Figure 2. Morphologies observed in 2wt% gels in water: (a) Interconnected ribbons and flexible sheets (cryo-TEM, bar = 500 nm). (b) close-up within the sheet-like assemblies: ribbons of thin 7 nm fibres assembled in parallel side-by-side (cryo-TEM, bar = 200 nm). (c) Interconnected ribbons and flexible sheets (TEM, bar = 1 µm). (d) random wormlike micelles (6 nm width) observed in the background just after shearing (cryo-TEM, Bar = 200 nm). (e) single and intertwined 10-13 nm helical fibres (cryo-TEM, bar = 200 nm). (f) Thick twin fibres (cryo-SEM, bar = 500 nm), width of one single fibre = 21 nm. (g) close-up within the helical fibres revealing the twisted assembly of 5 nm thick structures (bilayers) (TEM, negative staining, bar = 200 nm).

To better understand the effect of shear on those morphologies, cryo-TEM and TEM images were also recorded just after hydration of the solid and just after shearing. The microscopy (and also the SAXS, see below) of the solid hydrated for 16h at 2wt% in water and before shearing, already revealed the presence of 2D-sheets (Figure SI-3). Just after shearing, they were no longer observed. Instead, numerous small spots were seen on the whole grid, corresponding to dried wormlike micelles fragments (Figure SI-3). By using cryo-TEM, that avoids the formation of ambiguous drying figures, short and random 6-7 nm wide wormlike micelles were mainly observed (Figure 2-d).

The shear thus mainly broke and dispersed the sheets into individual and short wormlike micelles. After resting, these micelles re-assembled slowly into long wormlike micelles. Shearing also favoured their assembly side-by-side instead of randomly. It has been already shown that shear induced the formation of aligned wormlike micelles bundles in solutions of ionic surfactants. This association led to the formation of gels (transient or stable gels)[47]. However in the case of the gels of **3**, the structures observed are much longer (more than several microns long), and are organized in 7 nm thin sheets instead of bundles. They are able to sustain a gel stable over the long term reproducibly. These structures are also reminiscent of the unusual self-assembled lamellar plaques observed by Stupp et al. for amphiphilic peptides. These plaques split under shear into bundles of parallel fibres made of long cylindrical micelles [48]. Another example of long range and flexible 2D-self-assembly leading to gelation at relatively low concentration are lamellar hydrogels. They are also quite scarce in the literature. They have a purely lamellar organisation [49],[50]. This is not the case here. Besides, samples containing mainly the intertwined 10-13 nm helical fibres often failed to gel. Probably the helical fibres entanglements do not percolate through the whole sample or are not rigid, long and persistent enough to sustain a macroscopic gelation [51].

In contact with a surface (TEM grid), drying figures were formed. In the background of nearly all the TEM images of gelled samples, spots, but also holes with a typical jagged shape were observed (Figure 3-b). By AFM, the same jagged shapes were observed. They looked like the ones obtained for lipid bilayers dried on a surface. A constant thickness equal to 5-6 nm was measured (Figure 3-a). It matches well with the thickness of a single bilayer of gelator molecules with interdigitating alkyl chains and a polar head partly bended (Figure 5 and SI-15). Quite intriguingly, stacked layers displaying the same mosaic of jagged holes with this typical shape were observed also by cryo-SEM in addition to TEM and AFM (Figure 3-c).

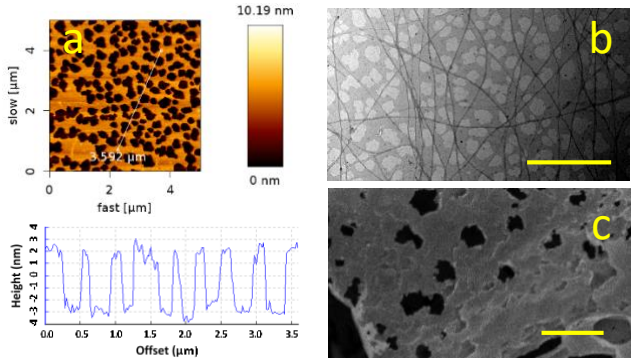

Figure 3. Figures with "jagged holes" formed after drying. (a) bilayer membrane on mica (AFM height and profile), (b) same membrane pattern on TEM grid, mixed with helical fibres (bar = 2 µm) (c) same pattern in cryo-SEM (bar = 1 µm).

Small Angle X-Ray Scattering (SAXS). SAXS investigation was performed to detail the changes in the morphology at the nanometre scale. SAXS curves of a 2% gel from 20°C to 70°C and the one of the freeze-dried solid are shown in Figure 4. The fit results are summarized in Table 1. All curves displayed two main features as the scattering vector, q, changes: (i) a power law trend, $I(q) \propto q^{-\alpha}$, in the low q region and, (ii) a broad interaction peak in the high q region. In gel sample, at 20°C, the whole scattering curve can be described by isolated sheets with 7.1 nm thickness to which two Gaussian peaks must be added in order to fully describe the high q region of the curve. These extra peaks correspond to a highly ordered state with a precise

correlation length very similar to a solid state. A progressive morphological change from sheets to cylinders with a diameter of about 10 nm and a length higher than 60 nm was observed from 20°C to 60°C. This transition was witnessed by the change in the low q region of the curves, i.e. the power law exponent went from about 2 to 1 as the temperature increased from 20°C to 60°C (see Table 1). In this region, the exponent scales with the dimensionality proper of the scattering object. 1-D morphologies (cylinders, rods, wires, etc.) give an exponent α of 1, while 2-D morphologies (disks, lamellae, etc.) result in an exponent of 2. In general values between 1 and 3 are usually associated to a mass fractal dimension where the limit of 3 is reached for full solids.

As already said, the high q region of the scattering curves is characterized by the presence of interaction peaks. In the freeze-dried solid, these peaks were ascribed to the coexistence of two polymorphs having two different organizations, one with a 6.3 nm spacing (l1, polymorph "L", more abundant) and the other with a 5.5 nm spacing (l2, polymorph "C"). Given the flexibility of the polar head, it is very likely that the molecule can take two distinct conformations (at least) giving rise to different bilayer packings (Figure 5). In modelling, the size of a fully extended molecule is 4.2 nm (SI-15). According to the models, bilayer thicknesses should be within the range from 8.4 nm (fully extended molecule and not interdigitated) to 4.3 nm (strongly bended polar head and interdigitated).

sample	T [°C]	α	Sheet Thickness [nm]	Cylinder Radius [nm]	Cylinder Length [nm]	l_1 [nm]	l_2 [nm]
solid	20	2.7±0.1	-	-	-	6.3±0.1	5.5±0.1
hydrated solid	20	2.3±0.1	7.4±0.2	-	-	6.8±0.3	5.5±0.3
gel 2%	20	2.1±0.1	7.1±0.5	-	> 60	6.7±0.3	5.5±0.3
"	30	1.9±0.1	7.1±0.6 (0.00035)	4.9±0.3 (0.000194)	> 60	6.9±0.2	5.6±0.2
"	40	1.8±0.1	7.1±0.6 (0.00027)	4.7±0.2 (0.00023)	> 60	7.0±0.2	5.4±0.2
"	50	1.4±0.1	-	5.0±0.1	> 60	7.0±0.2	5.6±0.2
"	60	1.1±0.1	-	4.5±0.1	32±5	7.0±0.4	5.6±0.4
"	50 back	1.1±0.1	-	5.0±0.2	> 60	-	5.5±0.2
"	20 back	1.3±0.1	-	5.8±0.2	> 60	-	5.8±0.2

Table 1. Results of fitting of SAXS curves: dry solid, solid after 24h hydration, gel 2wt%. α = power-law index in the q region between 0.009 $Å^{-1}$ and 0.03 $Å^{-1}$ for gel samples and 0.009 $Å^{-1}$ and 0.04 $Å^{-1}$ for the solid; l1 and l2 = spacing distances obtained from the Gaussian interaction peaks positions from $l = 2\pi/q$ (Table SI-14-2). In brackets are indicated the weight of each specie in the curve fits at 30 and 40°C.

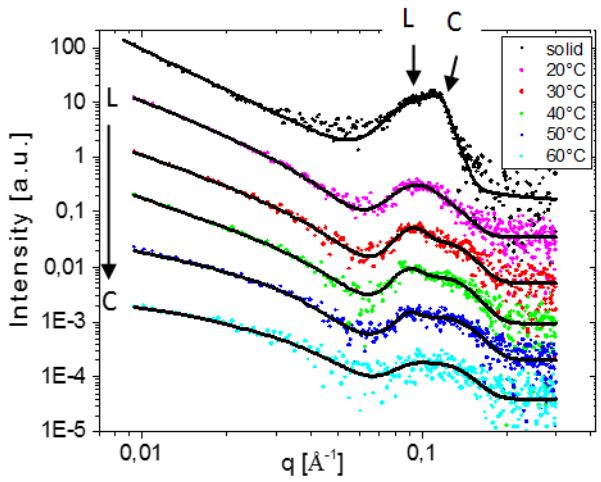

Figure 4. SAXS curves of the freeze-dried solid at 20°C (in black, at the top) and of a 2wt% gel prepared by shearing, then heated from 20°C to 60°C. L = sheets. C = cylinders

The dimensions measured by the interaction peaks are thus consistent with packings in which the alkyl chains are interdigitated and the polar head is more or less bended. Two examples of such packings providing a 6.5 nm (l1, extended) and a 5.3 nm (l2, partly bended) thickness are represented in Figure 5, keeping in mind that they are only illustrative [16,37,52]. The Gaussian interaction peaks were also seen in the gel samples at 0.91 nm^{-1} and 1.14 nm^{-1}. After hydration of the solid, without shear, the interaction peaks correspond to 6.8 nm (l1) and 5.5 nm (l2) spacing and shearing had no main effect at this microscopic scale (SI-14-1). The shift of l1 from 6.3 nm to 6.8 nm can be attributed to the intercalation of water in inter-lamellar spaces in the gel. These interaction peaks are indicative of the presence of solid-like inhomogeneities in the gel, after hydration. We assumed that the spacing measured in these solid-like inhomogeneities is directly related to the molecular organization once the aggregates are dispersed in the solution.

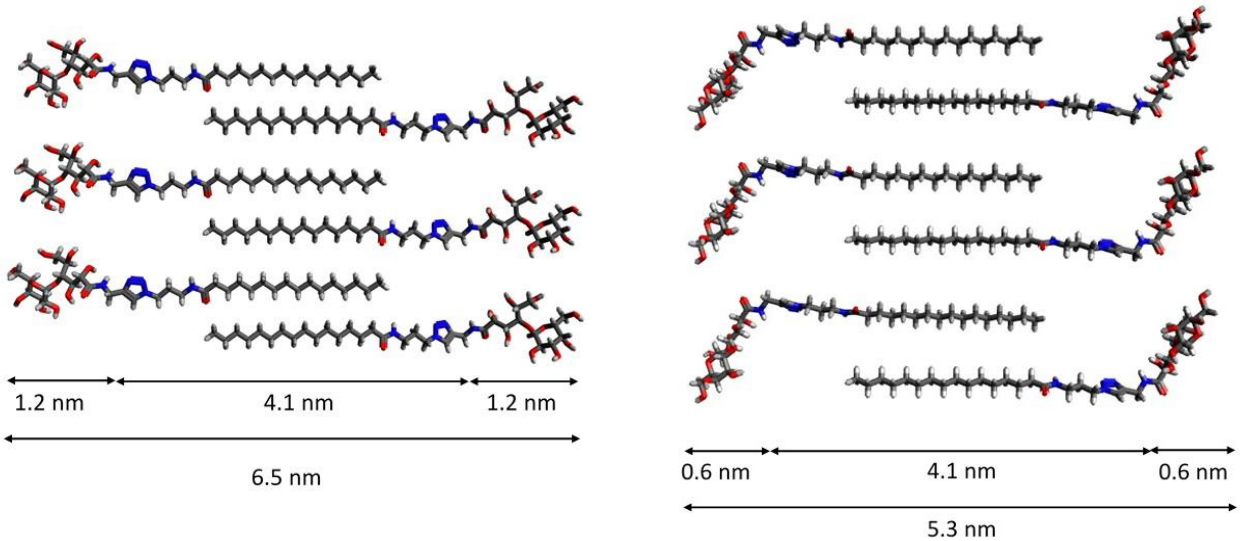

Figure 5. Illustration of possible conformations and packings of gelator ***3*** *. Up: a bilayer model with molecules in a fully extended conformation. Below: a bilayer model with molecules in a semi-bended conformation (molecular modelling suite Avogadro 1.1.1. with the Universal Force Field* [53]*. Colour code: C=grey, O=red, N=blue and H=white).*

From the analysis of the high q region, the ratio polymorph "L" / polymorph "C" is high in the solid. Conversely, in the gel sample this ratio is drastically reduced (almost five times less). This decrease is indicative of the fact that polymorph "L" in its hydrated form is more easily solubilised and provides the sheet-like aggregates at 20°C. Accordingly, the dimension of polymorph "L", l1 = 6.8-7.0 nm, is consistent with the mean thickness of the sheets (7.1 nm). And the dimension of the polymorph "C", l2 = 5.5 nm, appeared to be correlated to the cylinders in the gel state. Temperature did not influence much the peaks position, but it affected their ratio. Actually, the weight of the peak at 1.14 nm^{-1} increased with temperature and qualitatively the spectra moved at higher q values.

Discussion. From the results of the different experiments we concluded that after hydration, mainly two kinds of self-assembled objects are formed and dispersed in the solution: assemblies of cylindrical shape with a mean diameter around 10 nm (polymorph "C") and sheet-like assemblies with a sheet thickness of 7.1 nm (polymorph "L"). The sheet-like assemblies are the prevalent objects in solution at 20°C and in concentrated samples (2 wt%). They are the only ones detectable by scattering experiments. Their size is in good agreement with the one measured by cryo-TEM in the sheet-like assemblies made of long 7 nm-wide wormlike micelles, assembled parallel and side-by-side (Figure 2a-b). Besides, the 10-13 nm wide helical fibres found in cryo-TEM images (Figure 2e) match well the 10 nm diameter cylindrical objects detected in SAXS experiments above 30°C. The diameter of these cylinders is too big to correspond to cylindrical micelles. It can instead be explained by the twisting of bilayers with a 5-6 nm width observed by TEM (Figure 2g) and corresponding to the correlation length l2 (polymorph "C")[16,36,54]. The relative ratio sheet / cylinder in the low q region of the curves also decreases with temperature. The cylinders can be detected in scattering experiments only above 30°C, as their concentration increases, even though a fraction already exists at room temperature, as evidenced by the TEM images. The morphological transition from sheets to cylinders with temperature may be induced by a change in the molecular conformation. It is likely that the increase of temperature favours a bended conformation of the molecule, like in the polymorph "C", more stable and characterized by a shorter molecular spacing.

These transitions agree with DSC results and macroscopic observations. In particular, in DSC curves (Figure 1) a first peak at 20°C was observed, corresponding to the sheet-like structures (polymorph "L"). This transition is over at 30°C. The sheet-like objects coming from the polymorph "L" are responsible for the reproducible gelation after shearing, at the macroscopic scale. Sheets are the main species in the 2% gel after shearing, at 20°C, but are based on weak interactions. They disappear in favour of the more stable helical fibres, that exist in solution till 60°C. This assumption fits well with the second transition observed in DSC, at 55°C. After heating the sample over 30°C, gelled fragments were still observed floating in the solution: these fragments are sustained by the helical fibres. In some cases, these assemblies sustained also the macroscopic gelation, even in very diluted samples (0.5 %wt or less). Inthose samples only the transition at 55°C was observed (see SI-4). By heating up to 70°C and cooling back to 20°C, only the cylinders' signature was recovered, proving that this form corresponds to a thermodynamically controlled self-assembly, while the sheet-like aggregates are not. Instead they are closely related to the use of shear in concentrated samples.

Another point concerning the effect of heating is shown by the SAXS curve at 20°C relative to the heated sample, which failed to gel and gave a precipitate (SI-5). The curve displays an interaction peak corresponding to a 4.7 nm spacing (Figure SI-14-3), that is, lower compared with l1 and l2. It can correspond to a more bended conformation producing big aggregates which eventually precipitate. The presence of this third polymorph "P" is observed in the interaction peaks of samples once they have been cooled down from 70°C (see Figure SI-14-3, curves "50°C back" and "20°C back"). The formation of a third polymorph can explain the detrimental effect of heating on gel formation. This is why heating cannot be chosen as a robust protocol for producing the gels in a reproducible way.

Besides, low concentration gels at 0.5% were obtained in a reproducible manner by diluting and shearing the 2% samples. Their SAXS curves only displayed the signature of cylindrical structures (see Figure SI-14-2), indicating that the sheet-like structures did not withstand dilution. Using this method, the network of helical fibres produced was able to sustain the formation of a macroscopic gel.

E Rheology

Viscoelastic and thixotropic properties of gels at 2%wt have been measured. The frequency sweep from 10Hz to 0.01Hz displays a typical rheogram of gel, with G' > G" over the whole frequency range (Figure 6-a). G' is around 500 Pa, and G" between 30-60 Pa, featuring a quite fragile gel. The gel is thixotropic, namely after being sheared, it was able to recover its viscoelastic properties after resting. This point is illustrated in Figure 6-b-c. In Figure 6b, a gel (t=0, turned upside down) was vortexed for 15s. It flowed when turned upside down. One hour later, it had recovered its gel state and did not flow when turned upside down. In Figure 6-c, a gel (2%wt) was first sheared by passing through a needle, placed in the rheometer, and then G' and G" were monitored for 4h. G' in the destructured gel started at around 10Pa and progressively increased as the gel restructured up to 1000 Pa. The monitoring of the gel restructuration after shearing both with TEM and rheology has showed that the gel is dynamic, but with a very slow rate. According to macroscopic observations, this process of gel structuration with time kept on over several days and even weeks, since it was observed that some weak gels finally did not flow when turned upside down far later, after several weeks. From the microscopic point of view, the shear broke down the self-assembled structures formed after hydration into small objects (see section D "Microscopy", Figure 2d and SI-3). These fragments coalesced back slowly, into the long wormlike micelles assembled side-by-side, providing again the cross-linking points sustaining the gel network.

In relation to the slow dynamics of this restructuring, interestingly, it has been shown that the introduction of a sugar polar head in a dipeptide gelator (cyclo-L-Tyr-L-Lys) led to a strong slowing down of the gelation process[46]. But conversely, a nucleobase-derived gelator appended with a monosaccharide group displayed a quick gelation[28]. These different examples raise the question on how the introduction of sugar polar heads may affect more generally the self-assembly kinetics. Besides, in the case of LMW gels, thixotropy is known to be affected by the nature of self-assembled structures formed (e.g. spherulites versus fibres)[55]. In our case too, possibly only one of the two networks may sustain this rheological property. The viscoelastic changes with temperature have also been monitored by rheology, from 10 to 40°C. An abrupt decrease of the elastic modulus G' was observed from 25 to 30°C (Figure 6-d). The sharp increase of the phase from 5 to 70° in this temperature range evidenced the transition from

a gel to a sol. The elastic (G') and viscous (G") moduli crossed at 29°C. This measurement showed clearly the loss of the gel integrity in this range of temperature. It is consistent with the transition measured by DSC and SAXS and ascribed to the loss of the entangled sheets network of the polymorph "L".

a

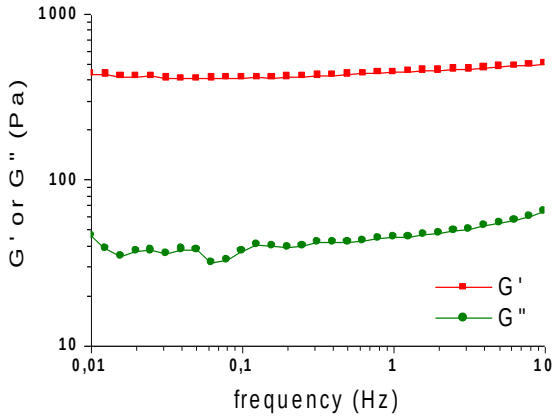

b

c

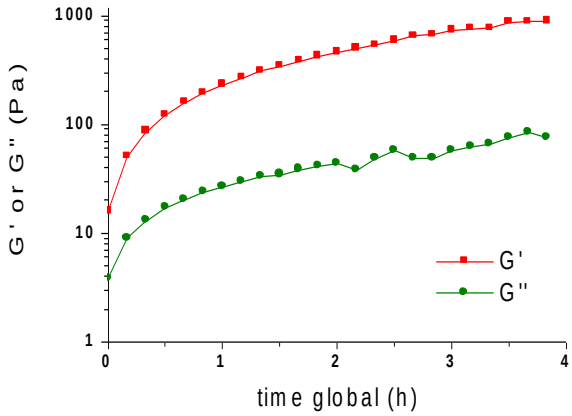

d

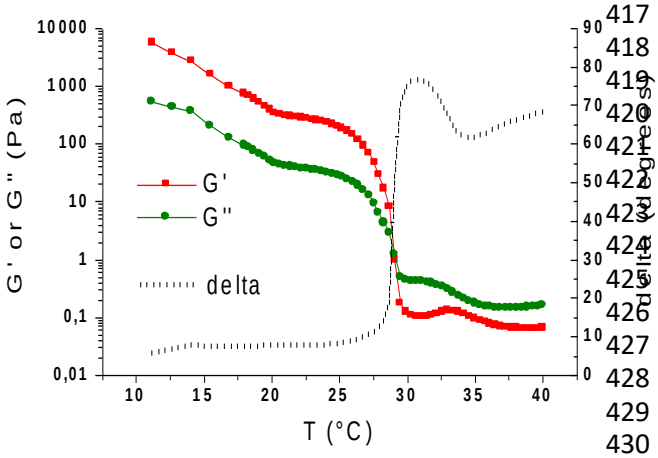

Figure 6. (a) Variation of G' (elastic modulus, squares) and G" (viscous modulus, circles) with frequency, at 1 Pa, 20°C. (b) Recovery of gel after shearing and resting for 1h. (c) Recovery of the elastic (G') and viscous (G") modulus with time, after shearing, measured at 0.1 Pa and 1 Hz. (d) Variation of G', G" and the phase (delta) with temperature, measured at 0.8 Pa and 1 Hz.

F Biocompatibility

Several molecular gels have been already tested as scaffold for cell culture, most of them belonging to the family of gelling peptides [2,56]. Compared with polymer gels, they can provide a different environment to cells, including different stiffness, a looser internal structure and higher clearance, that would help cells to grow through. Injectability, related to thixotropy, is also expected [2,7].

The gels of **3** have been tested as scaffold for cell culture with a neuronal cell line (Neuro 2A)[57]. After 3 days cultures, cell viability tests were performed (Figure 7). Cells adhered to the gel but only a poor number of viable cells was observed (<10%) (Figure 7-b). The gels did not appear suitable, whatever the method used for purifying the gelator or for preparing the gels. This result is in contrast with other low molecular weight hydrogels with close chemical structures on which cells were grown up to three days [58,59] or ten days [28]. Among the two networks sustaining the gel, one of them was dissolved at 37°C. It may have provided a high concentration of free gelator molecules, increasing the cytotoxicity. For comparison, the cytotoxicity of surfactants with close structure (sugar-triazole-fatty chain) was studied in ranges below 1 mmol/L, showing that surfactants with chains <6 carbons or >12 carbons had no toxicity on mammalian cells in this range [60]. In our case, gels at 0.1% correspond to a concentration of 1.4 mmol/L and gels at 1%, 14 mmol/L, far above the concentration range of this study. The molecular gels differ strongly from polymer gels on this point, since there is no bioavailability of small molecular units if biological degradation mechanisms do not provide fragments. This difference in the mechanism of gelation may affect the biocompatibility.

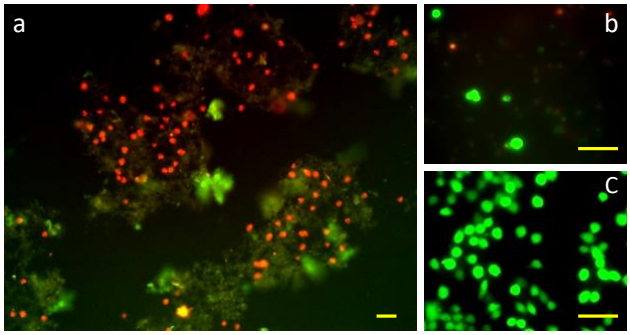

Figure 7. Cell viability assay. Neuro 2A cells have been cultured for 3 days on a 0.25%wt gel. Red staining indicates dead cells, green staining indicates live cells. The gel also appears by green autofluorescence. Fluorescence images at (a) low magnification and (b) high magnification. (c) Control cells after 3 days on cell culture plate. Scale bar 30 µm.

In addition, the mechanical strength of the scaffold is known to affect the cell survival, and in our gels, the dissolution of one of the two networks clearly decreased a lot the strength of the gel. Accordingly, we observed that the surviving cells were exclusively aggregated on the remaining gel fragments. It has been also demonstrated, in the case of amyloid peptides, that the nature of the polymorph, namely the way in which the molecules self-assemble, affected the cytotoxicity[40]. The same effects may occur in the case of supramolecular gelators. It points

out that the cell death is related not only to the chemical nature of the gel, but also to its mechanical properties and to subtle molecular organisation differences.

Conclusions

This new sugar-based gelator, despite an easy synthetic access, displayed quite a complex gelation behaviour in pure water due to polymorphism. The presence of two amides bonds, but separated from each other by a rigid spacer (triazole), forces the molecule to bend and favours the polymorphism. This observation may help the design of gelators. Without shearing, the gelation was capricious. Starting from 2wt% solutions and applying a strong shear enabled to get reproducible gelation. The resulting gels were diluted up to 0.25wt%. As a result of this method, the gel was sustained by a double network, one network of thin helical fibres with 10 nm of diameter and an unusual network of large interconnected 2D-sheets made of thin 7 nm wide wormlike micelles assembled side-by-side in parallel. The thermal transition of this second network was within the room temperature range. The resulting gel was partly thermoreversible and was thixotrope. Further heating, above 60°C, led to changes in the aggregation mode, giving shorter aggregates which could not sustain gelation and a precipitate was formed. This work illustrates that gelation can be highly dependent on the pathway used for the solubilisation and the dispersion of the gelator molecules. In our case, it involved both the hydration and solubilisation of the dry solid at room temperature in a range of concentration around 2wt%, before shearing. This work illustrates also that full solubilisation by heating, followed by cooling down can impair the self-assembly at the long range. It also showed that shearing induced the formation of new self-assembled and dynamic structures able to sustain a stable gel.

Acknowledgements

We acknowledge the following people for their technical assistance: TEM: I. Fourquaux, D. Goudounèche (CMEAB); V. Sartor, S. Gineste (IMRCP); NMR: P. Lavedan, M. Vedrenne (ICT). We acknowledge the European Union for funding (AFM, DSC) (FEDER 35477: "Nano-objets pour la biotechnologie") and The French National Research Agency (ANR) for financial support (ANR Neuraxe). We thank the Integrated Screening Platform of Toulouse (PICT, IBiSA) for providing access to HPLC equipment. LB and EF kindly acknowledge partial financial support from Consorzio per lo sviluppo dei Sistemi a Grande Interfase (CSGI). Thanks also to M. Mauzac for helpful discussions.

References

[1] R.G. Weiss, P. Terech, eds., Molecular gels: materials with self-assembled fibrillar networks, Springer, Dordrecht, 2006.

[2] X. Du, J. Zhou, J. Shi, B. Xu, Supramolecular Hydrogelators and Hydrogels: From Soft Matter to Molecular Biomaterials, Chem. Rev. 115 (2015) 13165–13307. doi:10.1021/acs.chemrev.5b00299.

[3] N. Zweep, J.H. van Esch, CHAPTER 1. The Design of Molecular Gelators, in: B. Escuder, J.F. Miravet (Eds.), RSC Soft Matter Ser., Royal Society of Chemistry, Cambridge, 2013: pp. 1–29. http://ebook.rsc.org/?DOI=10.1039/9781849737371-00001 (accessed April 4, 2016).

[4] A. Sorrenti, O. Illa, R.M. Ortuño, Amphiphiles in aqueous solution: well beyond a soap bubble, Chem. Soc. Rev. 42 (2013) 8200. doi:10.1039/c3cs60151j.

[5] M. de Loos, B.L. Feringa, J.H. van Esch, Design and Application of Self-Assembled Low Molecular Weight Hydrogels, Eur. J. Org. Chem. 2005 (2005) 3615–3631. doi:10.1002/ejoc.200400723.
[6] S.S. Babu, V.K. Praveen, A. Ajayaghosh, Functional π-Gelators and Their Applications, Chem. Rev. 114 (2014) 1973–2129.
[7] K.J. Skilling, F. Citossi, T.D. Bradshaw, M. Ashford, B. Kellam, M. Marlow, Insights into low molecular mass organic gelators: a focus on drug delivery and tissue engineering applications, Soft Matter. 10 (2014) 237–256. doi:10.1039/C3SM52244J.
[8] J. Raeburn, D.J. Adams, Multicomponent low molecular weight gelators, Chem Commun. 51 (2015) 5170–5180. doi:10.1039/C4CC08626K.
[9] D.J. Adams, P.D. Topham, Peptide conjugate hydrogelators, Soft Matter. 6 (2010) 3707. doi:10.1039/c000813c.
[10] C. Tomasini, N. Castellucci, Peptides and peptidomimetics that behave as low molecular weight gelators, Chem. Soc. Rev. 42 (2013) 156. doi:10.1039/c2cs35284b.
[11] K. Araki, I. Yoshikawa, Nucleobase-Containing Gelators, in: Low Mol. Mass Gelator, Springer Berlin Heidelberg, 2005: pp. 133–165. http://link.springer.com/chapter/10.1007/b107173 (accessed January 12, 2015).
[12] P. Dastidar, Supramolecular gelling agents: can they be designed?, Chem. Soc. Rev. 37 (2008) 2699. doi:10.1039/b807346e.
[13] L.E. Buerkle, S.J. Rowan, Supramolecular gels formed from multi-component low molecular weight species, Chem. Soc. Rev. 41 (2012) 6089. doi:10.1039/c2cs35106d.
[14] Y. Lin, C. Mao, Bio-inspired supramolecular self-assembly towards soft nanomaterials, Front. Mater. Sci. 5 (2011) 247–265.
[15] N.M. Sangeetha, U. Maitra, Supramolecular gels: Functions and uses, Chem. Soc. Rev. 34 (2005) 821. doi:10.1039/b417081b.
[16] L.A. Estroff, A.D. Hamilton, Water gelation by small organic molecules, Chem. Rev. 104 (2004) 1201–1218.
[17] F. Delbecq, Supramolecular gels from lipopeptide gelators: Template improvement and strategies for the in-situ preparation of inorganic nanomaterials and for the dispersion of carbon nanomaterials, Adv. Colloid Interface Sci. 209 (2014) 98–108. doi:10.1016/j.cis.2014.02.018.
[18] G. Fichman, E. Gazit, Self-assembly of short peptides to form hydrogels: Design of building blocks, physical properties and technological applications, Acta Biomater. 10 (2014) 1671–1682. doi:10.1016/j.actbio.2013.08.013.
[19] I.W. Hamley, Lipopeptides: from self-assembly to bioactivity, Chem Commun. 51 (2015) 8574–8583. doi:10.1039/C5CC01535A.
[20] E.K. Johnson, D.J. Adams, P.J. Cameron, Peptide based low molecular weight gelators, J Mater Chem. 21 (2011) 2024–2027. doi:10.1039/C0JM03099F.
[21] X.-Q. Dou, C.-L. Feng, Amino Acids and Peptide-Based Supramolecular Hydrogels for Three-Dimensional Cell Culture, Adv. Mater. (2017) 1604062. doi:10.1002/adma.201604062.
[22] T.K. Lindhorst, Essential of carbohydrate chemistry and biochemistry: [with 150 new exercises], 3., completely rev. and enl. ed., 1. reprint, Wiley-VCH, Weinheim, 2008.
[23] M.J. Clemente, R.M. Tejedor, P. Romero, J. Fitremann, L. Oriol, Maltose-based gelators having azobenzene as light-sensitive unit, RSC Adv. 2 (2012) 11419. doi:10.1039/c2ra21506c.
[24] M.J. Clemente, J. Fitremann, M. Mauzac, J.L. Serrano, L. Oriol, Synthesis and Characterization of Maltose-Based Amphiphiles as Supramolecular Hydrogelators, Langmuir. 27 (2011) 15236–15247. doi:10.1021/la203447e.
[25] M.J. Clemente, P. Romero, J.L. Serrano, J. Fitremann, L. Oriol, Supramolecular Hydrogels Based on Glycoamphiphiles: Effect of the Disaccharide Polar Head, Chem. Mater. 24 (2012) 3847–3858. doi:10.1021/cm301509v.
[26] M.J. Clemente, R.M. Tejedor, P. Romero, J. Fitremann, L. Oriol, Photoresponsive supramolecular gels based on amphiphiles with azobenzene and maltose or polyethyleneglycol polar head, New J. Chem. (2015). doi:10.1039/C4NJ02012J.
[27] G. Godeau, P. Barthélémy, Glycosyl-Nucleoside Lipids as Low-Molecular-Weight Gelators, Langmuir. 25 (2009) 8447–8450. doi:10.1021/la900140b.
[28] L. Latxague, M.A. Ramin, A. Appavoo, P. Berto, M. Maisani, C. Ehret, O. Chassande, P.

Barthélémy, Control of Stem-Cell Behavior by Fine Tuning the Supramolecular Assemblies of Low-Molecular-Weight Gelators, Angew. Chem. Int. Ed. 54 (2015) 4517–4521. doi:10.1002/anie.201409134.
[29] H.P.R. Mangunuru, J.R. Yerabolu, D. Liu, G. Wang, Synthesis of a series of glucosyl triazole derivatives and their self-assembling properties, Tetrahedron Lett. 56 (2015) 82–85. doi:10.1016/j.tetlet.2014.11.013.
[30] E. Carretti, V. Mazzini, E. Fratini, M. Ambrosi, L. Dei, P. Baglioni, P. Lo Nostro, Structure and rheology of gel nanostructures from a vitamin C-based surfactant, Phys Chem Chem Phys. 18 (2016) 8865–8873. doi:10.1039/C5CP07792C.
[31] A.G. Dal Bó, V. Soldi, F.C. Giacomelli, B. Jean, I. Pignot-Paintrand, R. Borsali, S. Fort, Self-assembled carbohydrate-based micelles for lectin targeting, Soft Matter. 7 (2011) 3453. doi:10.1039/c0sm01411g.
[32] A.G. Dal Bó, V. Soldi, F.C. Giacomelli, C. Travelet, R. Borsali, S. Fort, Synthesis, micellization and lectin binding of new glycosurfactants, Carbohydr. Res. 397 (2014) 31–36. doi:10.1016/j.carres.2014.07.021.
[33] G.C. Feast, T. Lepitre, X. Mulet, C.E. Conn, O.E. Hutt, G.P. Savage, C.J. Drummond, The search for new amphiphiles: synthesis of a modular, high-throughput library, Beilstein J. Org. Chem. 10 (2014) 1578–1588. doi:10.3762/bjoc.10.163.
[34] S. Díaz-Oltra, C. Berdugo, J.F. Miravet, B. Escuder, Study of the effect of polymorphism on the self-assembly and catalytic performance of an L-proline based molecular hydrogelator, New J. Chem. 39 (2015) 3785–3791. doi:10.1039/C5NJ00072F.
[35] V.J. Nebot, S. Díaz-Oltra, J. Smets, S. Fernández Prieto, J.F. Miravet, B. Escuder, Freezing Capture of Polymorphic Aggregates of Bolaamphiphilic L-Valine-Based Molecular Hydrogelators, Chem. – Eur. J. 20 (2014) 5762–5767. doi:10.1002/chem.201400346.
[36] J. Cui, A. Liu, Y. Guan, J. Zheng, Z. Shen, X. Wan, Tuning the Helicity of Self-Assembled Structure of a Sugar-Based Organogelator by the Proper Choice of Cooling Rate, Langmuir. 26 (2010) 3615–3622. doi:10.1021/la903064n.
[37] B.P. Krishnan, K.M. Sureshan, A Molecular-Level Study of Metamorphosis and Strengthening of Gels by Spontaneous Polymorphic Transitions, ChemPhysChem. 17 (2016) 3062–3067. doi:10.1002/cphc.201600590.
[38] S. Pan, S. Luo, S. Li, Y. Lai, Y. Geng, B. He, Z. Gu, Ultrasound accelerated gelation of novel l-lysine based hydrogelators, Chem. Commun. 49 (2013) 8045. doi:10.1039/c3cc44767g.
[39] A. Baral, S. Basak, K. Basu, A. Dehsorkhi, I.W. Hamley, A. Banerjee, Time-dependent gel to gel transformation of a peptide based supramolecular gelator, Soft Matter. 11 (2015) 4944–4951. doi:10.1039/C5SM00808E.
[40] A.T. Petkova, Self-Propagating, Molecular-Level Polymorphism in Alzheimer's -Amyloid Fibrils, Science. 307 (2005) 262–265. doi:10.1126/science.1105850.
[41] J. Raeburn, A. Zamith Cardoso, D.J. Adams, The importance of the self-assembly process to control mechanical properties of low molecular weight hydrogels, Chem. Soc. Rev. 42 (2013) 5143. doi:10.1039/c3cs60030k.
[42] V.J. Nebot, D.K. Smith, CHAPTER 2. Techniques for the Characterisation of Molecular Gels, in: B. Escuder, J.F. Miravet (Eds.), RSC Soft Matter Ser., Royal Society of Chemistry, Cambridge, 2013: pp. 30–66. http://ebook.rsc.org/?DOI=10.1039/9781849737371-00030 (accessed April 4, 2016).
[43] J.T. van Herpt, M.C.A. Stuart, W.R. Browne, B.L. Feringa, Mechanically Induced Gel Formation, Langmuir. 29 (2013) 8763–8767. doi:10.1021/la401286a.
[44] X. Cai, Y. Wu, L. Wang, N. Yan, J. Liu, X. Fang, Y. Fang, Mechano-responsive calix[4]arene-based molecular gels: agitation induced gelation and hardening, Soft Matter. 9 (2013) 5807. doi:10.1039/c3sm50577d.
[45] A. Reddy M, A. Srivastava, Mechano-responsive gelation of water by a short alanine-derivative, Soft Matter. 10 (2014) 4863. doi:10.1039/c4sm00710g.
[46] Z. Xie, A. Zhang, L. Ye, X. Wang, Z. Feng, Shear-assisted hydrogels based on self-assembly of cyclic dipeptide derivatives, J. Mater. Chem. 19 (2009) 6100. doi:10.1039/b912020c.
[47] J.J. Cardiel, A.C. Dohnalkova, N. Dubash, Y. Zhao, P. Cheung, A.Q. Shen, Microstructure and rheology of a flow-induced structured phase in wormlike micellar solutions, Proc. Natl. Acad. Sci. 110 (2013) E1653–E1660. doi:10.1073/pnas.1215353110.

[48] S. Zhang, M.A. Greenfield, A. Mata, L.C. Palmer, R. Bitton, J.R. Mantei, C. Aparicio, M.O. de la Cruz, S.I. Stupp, A self-assembly pathway to aligned monodomain gels, Nat Mater. 9 (2010) 594–601. doi:10.1038/nmat2778.
[49] H.E. Warriner, S.H.J. Idziak, N.L. Slack, P. Davidson, C.R. Safinya, Lamellar Biogels: Fluid-Membrane-Based Hydrogels Containing Polymer Lipids, Science. 271 (1996) 969–973. doi:10.1126/science.271.5251.969.
[50] J. Niu, D. Wang, H. Qin, X. Xiong, P. Tan, Y. Li, R. Liu, X. Lu, J. Wu, T. Zhang, W. Ni, J. Jin, Novel polymer-free iridescent lamellar hydrogel for two-dimensional confined growth of ultrathin gold membranes, Nat. Commun. 5 (2014). doi:10.1038/ncomms4313.
[51] S.R. Raghavan, J.F. Douglas, The conundrum of gel formation by molecular nanofibers, wormlike micelles, and filamentous proteins: gelation without cross-links?, Soft Matter. 8 (2012) 8539. doi:10.1039/c2sm25107h.
[52] N. Baccile, A.-S. Cuvier, S. Prévost, C.V. Stevens, E. Delbeke, J. Berton, W. Soetaert, I.N.A. Van Bogaert, S. Roelants, Self-Assembly Mechanism of pH-Responsive Glycolipids: Micelles, Fibers, Vesicles, and Bilayers, Langmuir. 32 (2016) 10881–10894. doi:10.1021/acs.langmuir.6b02337.
[53] M.D. Hanwell, D.E. Curtis, D.C. Lonie, T. Vandermeersch, E. Zurek, G.R. Hutchison, Avogadro: an advanced semantic chemical editor, visualization, and analysis platform, J. Cheminformatics. 4 (2012) 17. doi:10.1186/1758-2946-4-17.
[54] L. a. Estroff, L. Leiserowitz, L. Addadi, S. Weiner, A. d. Hamilton, Characterization of an Organic Hydrogel: A Cryo-Transmission Electron Microscopy and X-ray Diffraction Study, Adv. Mater. 15 (2003) 38–42. doi:10.1002/adma.200390004.
[55] X. Huang, S.R. Raghavan, P. Terech, R.G. Weiss, Distinct Kinetic Pathways Generate Organogel Networks with Contrasting Fractality and Thixotropic Properties, J. Am. Chem. Soc. 128 (2006) 15341–15352. doi:10.1021/ja0657206.
[56] J. Zhou, J. Li, X. Du, B. Xu, Supramolecular biofunctional materials, Biomaterials. 129 (2017) 1–27. doi:10.1016/j.biomaterials.2017.03.014.
[57] A. Béduer, I. Gonzales-Calvo, C. Vieu, I. Loubinoux, L. Vaysse, Investigation of the Competition Between Cell/Surface and Cell/Cell Interactions During Neuronal Cell Culture on a Micro-Engineered Surface, Macromol. Biosci. 13 (2013) 1546–1555. doi:10.1002/mabi.201300202.
[58] W. Wang, H. Wang, C. Ren, J. Wang, M. Tan, J. Shen, Z. Yang, P.G. Wang, L. Wang, A saccharide-based supramolecular hydrogel for cell culture, Carbohydr. Res. 346 (2011) 1013–1017. doi:10.1016/j.carres.2011.03.031.
[59] X. Li, Yi Kuang, J. Shi, Y. Gao, H.-C. Lin, B. Xu, Multifunctional, Biocompatible Supramolecular Hydrogelators Consist Only of Nucleobase, Amino Acid, and Glycoside, J. Am. Chem. Soc. 133 (2011) 17513–17518. doi:10.1021/ja208456k.
[60] E.D. Oldham, S. Seelam, C. Lema, R.J. Aguilera, J. Fiegel, S.E. Rankin, B.L. Knutson, H.-J. Lehmler, Synthesis, surface properties, and biocompatibility of 1,2,3-triazole-containing alkyl β-d-xylopyranoside surfactants, Carbohydr. Res. 379 (2013) 68–77. doi:10.1016/j.carres.2013.06.020.